Membraneless fuel cells using Pt-Ru-Sn/C catalysts for methanol oxidation

S.M. Nayeemunisa[1a], S. Kiruthika[2b], K. Ponmani[3c], S. Durga[3d]
and B. Muthukumaran[*3]

[1]*Department of Chemistry, Justice Basheer Ahmed Sayeed College for Women, Chennai, 600 018, India*
[2]*Department of Chemical Engineering, SRM University, Chennai, 603 203, India*
[3]*Department of Chemistry, Presidency College, Chennai, 600 005, India*

Abstract. In the present work, the continuous flow operation of membraneless methanol fuel cell (MLMFC) using Pt-Ru-Sn/C electrocatalysts with different atomic ratios were prepared by alcohol-reduction process. In this membraneless fuel cell, methanol is used as a fuel, sodium percarbonate is used as an oxidant and sulphuric acid is used as the electrolyte. Sodium percarbonate affords hydrogen peroxide in aqueous medium. The synthesized electrocatalysts were characterized by transmission electron microscopy (TEM), energy dispersive X-ray spectroscopy (EDX) and X-ray diffraction (XRD) analyses. The electrocatalytic activities of the catalysts were characterized by cyclic voltammetry (CV) and chronoamperometry (CA). During the experiments performed on single membraneless fuel cells, Pt-Ru-Sn/C (70:20:10) performed better among all the catalysts prepared with power density of 36.5 mWcm^{-2}. The better performance of ternary Pt-Ru-Sn/C catalysts may be due to the formation of a ternary alloy and the smaller particle size.

Keywords: renewable energy; environment-friendly sodium percarbonate; membraneless methanol fuel cells; ternary catalysts; portable power applications

1. Introduction

Pollution free renewable energy is the goal to meet up the global growing energy requirement. Fuel cell technologies have drawn significant attention for high efficiency in direct conversion of chemical energy into electrical energy, as well as environmental compatibility. Many different types of fuel cells are currently under development, with a variety of targeted applications ranging from miniature power supplies to large-scale power plants. Small fuel cells have received much interest in recent years as potential power supplies for the next generation of portable electronic

---

∗Corresponding author, Professor, E-mail: dr.muthukumaran@yahoo.com
[a]Ph.D., E-mail: nayeemunisa27@gmail.com
[b]Ph.D., E-mail: kiruthika.s@ktr.srmuniv.ac.in
[c]Ph.D. Student, E-mail: ponmani_k@yahoo.co.in
[d]Ph.D. Student, E-mail: durgasrika@gmail.com

devices.

One class of microstructured power supply is microfluidic fuel cells, also called laminar flow-based fuel cells and membraneless fuel cells. A membraneless microfluidic fuel cell is a device in which two aqueous streams flow laminarly in the absence of a physical membrane without turbulent mixing (Choban *et al*. 2005).

Microfluidic membraneless fuel cells avoid many of the issues associated with polymer electrolyte membrane-based fuel cells such as humidification, membrane degradation, water management, and fuel crossover (Carrette *et al*. 2000). Moreover, miniaturization of membraneless fuel cells has drawn significant interest because of potential advantages: compact design, high-energy conversion efficiency, low operating temperature, environmental-friendly emissions, use of both metallic and biological catalysts and elimination of moving parts (Ferigno *et al*. 2002). However, their practical applications are hindered by the sluggish electrochemical reaction on the catalytic surface, formation of depletion boundary layers close to the catalyst-covered electrodes and poor fuel utilization (Fig. 1).
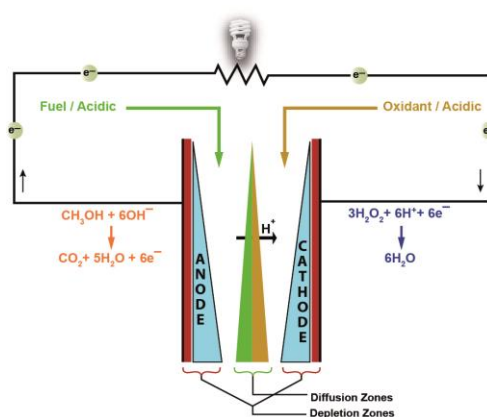
Fig. 1 A cross-section of a channel showing depletion boundary layer over anode and cathode metal catalysts and an interdiffusion zone at the liquid-liquid interface with vertical electrodes on the side walls

In the present work, we study the fabrication and performance of an E-shaped (Arun *et al*. 2014, Gowdhamamoorthi *et al*. 2014) membraneless methanol fuel cell (MLMFC) using laminar flow-based configuration that fulfill the aforementioned requirements. Methanol is considered as one of the most promising combustible materials used in fuel cells, because of its high-energy storage (5,019 A h Kg^{-1}), low toxicity, large-scale production from biomass, easy storage and transportation, and facile electro-oxidation on Pt catalyst. It is renewable, and its complete oxidation to CO_2 and H_2O produces a high yield of 6 electrons per molecule in acid electrolyte as shown in Eq. (1).

$$CH_3OH + H_2O \rightarrow CO_2 + 6H^+ + 6e^- \qquad (1)$$

However, methanol electro-oxidation on pure platinum encounters many problems such as the difficulties in adsorption and dehydrogenation of the methanol molecule and the formation of CO-intermediates that poison the Pt anode catalysts. The slow kinetics of the methanol electro-

oxidation reaction (MOR) on Pt anode diminishes the overall performance of the MLMFC system. There have been considerable efforts to develop alternative anode electrocatalysts that offer high catalytic activity for MOR. For example, alloying of Pt with other elements such as Ru, Sn, Mo, W, Pd, Ni, Rh and Ir have been studied, and among them, Ru and Sn have shown the best catalytic effect on MOR (Chan *et al*. 2004, Casado *et al*. 2004, Xiong *et al*. 2002). The second metal of the co-catalysts shows bifunctional mechanism and has a ligand effect (Gasteiger *et al*. 1993, Yajima *et al*. 2004). Nevertheless, it is still an ongoing task to improve the performance of Pt-Ru and Pt-Sn anode catalysts to a level suitable for commercialization.

The Pt-Ru/C and Pt-Sn/C electrocatalysts' performance also depends on the preparation procedures and their atomic ratios. (Jiang *et al*. 2005) prepared Pt-Sn alloy by polyol method, which inhibited the hydrogen adsorption/desorption process. (Song *et al*. 2005) verified that the Pt-Sn catalyst presents greater selectivity for the oxidation of this alcohol compared with Pt alone via gas chromatography. (Neto *et al*. 2007) investigated methanol electro-oxidation using carbon-supported Pt-Sn catalysts prepared by alcohol reduction method. Recently, (Mitra *et al*. 2015) synthesized the carbon-polyaniline supported Pt-Ru and Pt-Sn electrocatalysts by the impregnation method. They observed that the CO tolerance and stability of Pt-Sn (70:30)/C-PANI was considerably higher than that of Pt-Ru/C in methanol electro-oxidation reaction.

To further improve Pt-Ru/C and Pt-Sn/C electrocatalysts activity, a third metal is introduced into their composition, which helps to enhance the dehydrogenation reaction and the CO tolerance of the catalysts during the oxidation of methanol. The enhanced activity of the ternary catalyst is due to the promoting effect of the second or third elements added to Pt. Moreover, the main advantage of the introduction of the third metal is the reduction of the oxidation potential of small organic molecules, coupled with the rise in current density. In the present study, we evaluated the catalytic activity for the methanol electro-oxidation reaction by incorporating a third metal Sn to the Pt-Ru catalyst on a carbon support in membraneless methanol fuel cell (MLMFC). The performance of the Pt-Ru-Sn/C catalyst was compared with that of the Pt-Ru/C and Pt-Sn/C catalysts obtained by the alcohol-reduction method.

2. Experimental

2.1 Material

The metal precursors used for the preparation of electrocatalysts were $H_2PtCl_6.6H_2O$ (from Aldrich), $RuCl_3.3H_2O$ (from Merck), and $SnCl_2.2H_2O$ (from Alfa Aesar). Vulcan XC-72R carbon black (from Cabot Corp.,) was used as a support for the catalysts. Graphite plates (from E-TEK) were used as substrates for the catalyst to prepare the electrodes. Ethylene glycol (from Merck) was used as the solvent and reduction agent. Nafion[®] (DE 521, DuPont USA) dispersion was used to make the catalyst ink. Methanol (from Merck), sodium percarbonate (from Aldrich) and H_2SO_4 (from Merck) were used as the fuel, the oxidant and as the electrolyte for electrochemical analysis, respectively. All the chemicals were of analytical grade. Pt/C (40-wt%, from E-TEK) was used as the cathode catalyst.

2.2 Preparation of electrocatalysts

Carbon supported ternary Pt-Ru-Sn catalysts with different atomic ratios were synthesized by

the alcohol-reduction process (Spinace *et al*. 2005). Initially, the precursors were suspended in ethylene glycol and water (75/25 v/v), followed by the addition of carbon support. The resulting mixtures were treated in an ultrasound bath and were refluxed for 3 h under the open atmosphere. Then the solution was made alkaline (about pH 12) and heated at 140°C for 3 h under agitation to enable the metal's reduction. Finally, the precipitate was collected by filtration, washed with ultrapure water (Millipore MilliQ, 18 MΩ cm), and dried at 70°C for 2 h. For comparison, the monometallic Pt/C, and bimetallic Pt-Ru/C and Pt-Sn/C catalysts were synthesized under the same conditions. The electrocatalytic mixtures and atomic ratios were Pt/C (100), Pt-Ru/C (50:50), Pt-Sn/C (50:50), Pt-Ru-Sn/C (70:10:20), Pt-Ru-Sn/C (70:15:15) and Pt-Ru-Sn/C (70:20:10). The nominal loading of metals in the electrocatalysts was 40%wt and rest 60%wt was carbon.

2.3 Preparation of the working electrode

The catalyst ink was prepared by mixing 50 mg of carbon supported catalyst powder and 1 mL of Nafion solution (5 wt.%) in 5 mL ultrapure millipore water. 3 μL of ultrasonically homogenized ink was deposited onto a freshly polished glassy-carbon electrode before each experiments and the solvent was then evaporated in open air at room temperature. The loading of metal on the working electrode was 0.28 mg_{metal} cm^{-2}.

2.4 Physical characterization

The morphology, particle size distribution and mean particle size of the dispersed catalysts were examined by transmission electron microscopy (TEM) (Philips CM 12 Transmission Electron Microscope). The crystal structure of the synthesized electrocatalysts was characterized by powder *X*-ray diffraction (XRD) using a Rigaku multiflex diffractometer (model RU-200 B) with Cu-$K_{\alpha1}$ radiation source ($\lambda_{K\alpha1}$=1.5406 A°) operating at room temperature. The tube current was 40 mA with a tube voltage of 40 kV. The 2θ angular regions between 20° and 90° were recorded at a scan rate of 5° min^{-1}. The mean particle size analyzed from TEM is verified by determining the crystallite size from XRD pattern using Scherer formula. Pt (2 2 0) diffraction peak was selected to calculate crystallite size and lattice parameter of platinum. According to Scherrer's equation (Radmilovic *et al*. 1995)

$$d = \frac{0.9\lambda_{K\alpha1}}{\beta_{2\theta}\cos\theta_{max}} \tag{2}$$

where *d* is the average crystallite size, θ_{max} is the angle at the position of the peak maximum, $\beta_{2\theta}$ is the width of the peak (in radians), 0.9 is the shape factor for spherical crystallite and $\lambda_{K\alpha1}$ is the wavelength of *X*-rays used. The lattice parameters of the catalysts were estimated according to equation 3

$$a = \frac{\sqrt{2}\,\lambda_{K\alpha1}}{\mathrm{Sin}\,\theta_{max}} \tag{3}$$

where *a*, is the lattice parameter (nm) and all the other symbols have the same meanings as in Eq. 2 (Beyhan *et al*. 2013). The atomic ratio of the catalysts was determined by an energy dispersive X-ray (EDX) analyzer, which was integrated with the TEM instrument.

2.5 Electrochemical measurements

Electrochemical studies of the electrocatalysts were carried out using the thin porous coating technique (Colmati *et al.* 2007). All electrochemical measurements were performed on an electrochemical workstation (CH Instruments, model CHI6650, USA) interfaced with a personal computer using the CHI software, at room temperature. A common three-electrode electrochemical cell using cyclic voltammetry (CV) and chronoamperometry (CA) techniques was used for the measurements. Catalyst coated glassy carbon electrode (GCE, 3 mm diameter and 0.071 cm^2 of electrode area, from CHI, USA) was used as the working electrode and platinum foil was used as the counter electrode. Ag/AgCl in saturated KCl was used as the reference electrode. For assessing the electrocatalytic activity of the working electrode, cyclic voltammetry was obtained in 0.5 M H$_2$SO$_4$ or 1 M CH$_3$OH/0.5 M H$_2$SO$_4$ solution with a scan rate of 0.5 Vs^{-1}. For the durability test, the chronoamperometric experiments were carried out at 0.1 V for 6000 s in the same electrolyte. Before each measurement, the solution was purged with high-purity nitrogen gas for at least 30 min to ensure oxygen-free measurements.

2.6 Single cell test

In the present study, we fabricated the membraneless methanol fuel cell using laminar flow-based fuel cell configuration. In this membraneless fuel cell, methanol is used as a fuel, sodium percarbonate is used as an oxidant and sulphuric acid is used as the electrolyte. Sodium percarbonate (2Na$_2$CO$_3$.3H$_2$O$_2$) is a cheap, environment friendly, nontoxic, and large-scale industrial chemical, primarily used as a source of 'active oxygen' in detergents and as a mild antiseptic. Percarbonate is a convenient source of H$_2$O$_2$ (Cotton *et al.* 1988; Karunakaran *et al.* 2002), commercially, industrially and also in the laboratory as demonstrated in Eq. (4).

$$2Na_2CO_3.3H_2O_2 \rightarrow 2Na_2CO_3 + 3H_2O_2 \qquad (4)$$

In fact, the compound is sodium percarbonate sesquiperhydrate and it contains hydrogen peroxide as such in the solid state.

In MLMFC, the aqueous fuel and oxidant streams flow in parallel in a single microchannel with the anode and cathode on opposing sidewalls (Fig. 2). Graphite plates of one mm thickness served as current collectors and catalyst support structures. The anode catalysts with different atomic ratios were coated onto the graphite plates. For single cell, the anode catalysts were prepared as follows: The catalyst ink was prepared by mixing 100 μL of Nafion (5 wt.% from DuPont) solution, 1 mL of isopropanol and 15 mg of catalytic powder. This mixture was then brushed on a graphite plate in 3 cm^2 areas and dried at 100°C for 30 min to give an approximate total metal loading of 2 mg cm^{-2} on the anode. The catalysts tested on the anode side were Pt/C (100), Pt-Ru/C (50:50), Pt-Sn/C (50:50), Pt-Ru-Sn/C (70:10:20), Pt-Ru-Sn/C (70:15:15) and Pt-Ru-Sn/C (70:20:10). On the cathode side, Pt/C (100) with catalyst loading 2 mg cm^{-2} was used in all experiments.

The two catalyst-coated graphite plates were aligned to form a channel with 0.1 cm electrode-to-electrode distance (width), a 3 cm length, and a 0.1 cm height. The anolyte (fuel and electrolyte) and catholyte (oxidant and electrolyte) streams flow in a laminar fashion over the anode and cathode, respectively. The electrode area along a microchannel wall between the inlets and the outlet (3 cm long and 0.1 cm wide) was used as the geometric surface area of the electrodes in this study (0.3 cm^2). The design is described in detail elsewhere (Choban *et al.* 2004, Jayashree *et al.*
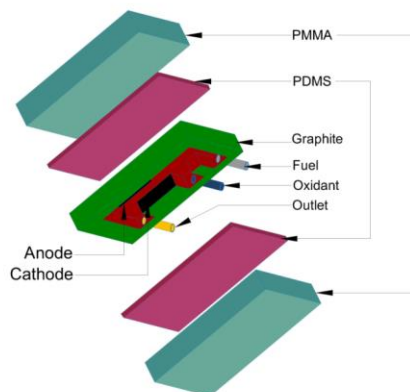
Fig. 2 Schematic of the *E*-shaped membraneless laminar flow-based fuel cell with catalyst-coated graphite plates molded with poly(dimethylsiloxane) (PDMS) and sealed with poly (methylmethacrylate) (PMMA)

2010). The anolyte used in the anode side was 1.0 M methanol + 0.5 M H_2SO_4 and the catholyte used in the cathode side was 0.1 M percarbonate + 0.5 M H_2SO_4. The flow rate of each of the streams was 0.3 mL min^{-1} (total flow rate of 0.6 mL min^{-1}). The MLMFC was operated at room temperature. The current-voltage characteristics of MLMFC were measured using an electrochemical workstation (CH Instruments, model CHI6650, USA) and the data was verified using a multi-meter (MASTECH® MAS830L).

3. Results and discussions

3.1 Physical characterization

3.1.1 X-ray diffraction (XRD)

The XRD patterns of the prepared Pt-Ru/C (50:50), Pt-Sn/C (50:50), Pt-Ru-Sn/C (70:10:20), Pt-Ru-Sn/C (70:15:15) and Pt-Ru-Sn/C (70:20:10) catalysts are shown in Fig. 3. The diffraction peaks seen in all the diffraction patterns at around 25-30° are associated with (0 0 2) plane of hexagonal structure of Vulcan XC-72R carbon support. The diffractogram of Pt-Ru/C electrocatalyst show peaks at around 40°, 47°, 67° and 82°, which are associated with the (1 1 1), (2 0 0), (2 2 0) and (3 1 1) crystalline planes respectively, of the face centered cubic (fcc) structure characteristic of platinum and platinum alloys. No peaks corresponding to a metallic ruthenium or the ruthenium oxides were detected in the Pt-Ru-Sn catalysts, but their presence cannot be discarded because they may be present in a very small particle size or even in an amorphous form (Spinace *et al*. 2004). The Pt-Sn/C electrocatalyst also showed the peaks characteristic of the fcc structure of platinum and platinum alloys similar to Pt-Ru/C electrocatalysts. However, in this sample two additional peaks were observed at 34° and 52° that were identified as a SnO_2 phase (Spinace *et al*. 2005). The fcc lattice parameters were evaluated from the angular position of the (2 2 0) peaks and the calculated value for Pt-Ru/C electrocatalyst (0.3891 nm) was smaller than that of Pt/C electrocatalyst (0.3912 nm), indicating a contraction of the lattice and a Pt and Ru alloy to some extent. For Pt-Sn/C electrocatalyst the fcc lattice parameter measured (0.3982 nm) was larger

Table 1 The EDX composition, lattice parameters, and the particle size obtained for different atomic ratios of electrocatalysts

	Nominal atomic ratio			EDX Atomic ratio			Lattice parameter (nm)	Crystallite size (D) (nm)	Particle size from TEM (nm)
	Pt	Sn	Ru	Pt	Sn	Ru			
Pt-Sn/C	50	50	-	53	47		0.3982	4.0	3.7
Pt-Ru/C	50	-	50	54	46		0.3891	3.9	3.6
Pt-Ru-Sn/C	70	10	20	68	13	19	0.3937	3.0	2.5
Pt-Ru-Sn/C	70	15	15	72	16	12	0.3905	2.8	2.2
Pt-Ru-Sn/C	70	20	10	73	18	9	0.3886	2.5	2.0
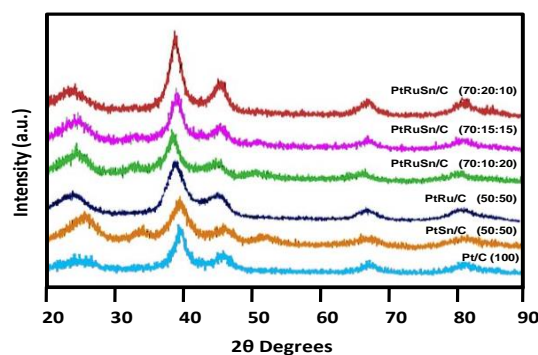
Fig. 3 *X*-ray diffraction patterns of Pt-Ru-Sn/C (70:10:20), Pt-Ru-Sn/C (70:15:15) and Pt-Ru-Sn/C (70:20:10), Pt-Sn/C (50:50), Pt- Ru/C (50:50) and Pt/C (100) catalysts

than the one obtained for Pt/C electrocatalyst, due to a lattice expansion after alloying, indicating that part of Sn was incorporated in the fcc structure of Pt. The fcc lattice parameters calculated for Pt-Ru-Sn/C electrocatalysts were: Pt-Ru-Sn/C 70:10:20 (0.3937 nm), Pt-Ru-Sn/C 70:15:15 (0.3905 nm) and Pt-Ru-Sn/C 70:20:10 (0.3886 nm). Compared to Pt/C electrocatalyst the fcc lattice parameter was increased in Pt-Ru-Sn/C (7010:20) electrocatalyst but decreased in Pt-Ru-Sn/C (70:20:10) electrocatalyst. The difference of lattice parameters and the shift of (2 2 0) plane indicate interactions between Pt, Ru, and Sn. The peaks of the SnO_2 phase at $34°$ and $52°$ were clearly observed for Pt-Ru-Sn/C (70:10:20) and (70:15:15), while for Pt-Ru-Sn/C (70:20:10) only the peaks characteristic of the Pt fcc structure were observed. The average particle size was estimated using the Scherrer equation (Table 1). The particle sizes for Pt-Ru/C, Pt-Sn/C, and Pt-Ru-Sn/C electrocatalysts were in the range of 2.5-4.0 nm.

3.1.2 Transmission electron microscopy (TEM)
The TEM images of the Pt/C, Pt-Sn/C, Pt-Ru/C and Pt-Ru-Sn/C catalysts are presented in Fig. 4. Fig. 4(a)-(d) indicates that catalysts consist of nano sized metal particles, uniformly dispersed on carbon support. It can be seen from the images that the metal particle sizes of each sample are less than 5 nm, and they are of spherical shape and slightly agglomerated. Agglomeration might be ascribed to fast reduction process (Zhou *et al*. 2005). In comparison to Pt-Sn/C (50:50) and Pt-Ru-Sn/C (70:10:20) the mean particle size of Pt-Ru-Sn/C (70:15:15) and Pt-Ru-Sn/C (70:20:10) were smaller. The particle size distribution of these catalysts is shown in Table 1 in accordance to the
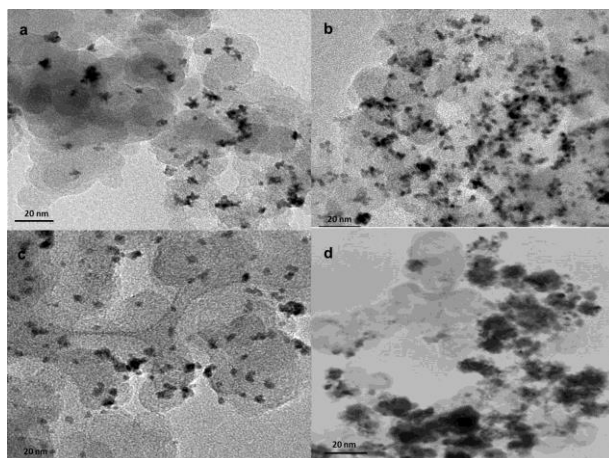
Fig. 4 TEM images of (a) Pt/C, (b) Pt-Sn/C, (c) Pt-Ru/C and (d) Pt-Ru-Sn/C catalysts
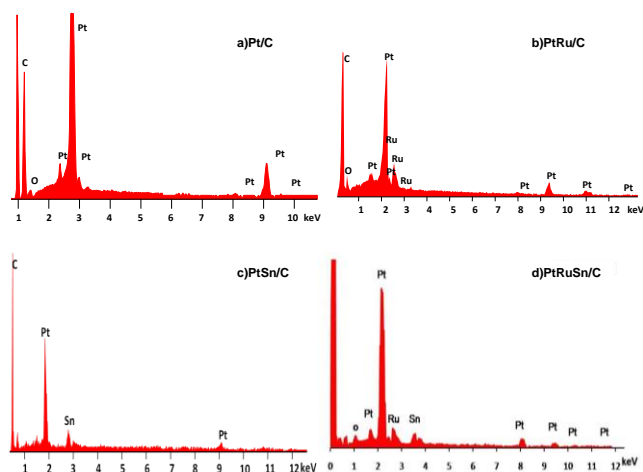
Fig. 5 EDX spectra of (a) Pt/C, (b) Pt-Ru/C, (c) Pt-Sn/C and (d) Pt-Ru-Sn/C catalysts

TEM images. The mean particle size found by TEM image and XRD analysis were similar. Further, it was observed that the particle size of Pt-Ru/C (50:50) was similar to that of Pt-Sn/C (50:50).

3.1.3 Energy dispersive X-ray (EDX) analysis

The EDX analyses of all the Pt-Sn/C, Pt-Ru/C, and Pt-Ru-Sn/C catalysts are shown in Fig. 5. Fig. 5(a)-(d) indicates the presence of Pt, Ru and carbon; Pt, Sn and carbon; and both the combinations of Pt, Ru, Sn, and carbon, respectively. The EDX results are shown in Table 1. The catalysts prepared had the desired elements with some variation in composition. The EDX results of the binary Pt-Sn/C and Pt-Ru/C and the ternary Pt-Ru-Sn/C catalysts are very close to the nominal values, which indicate that the metals were loaded onto the carbon support without obvious loss.

3.2 Electrochemical characterization

3.2.1 Cyclic voltammetry (CV)

Fig. 6(a) shows the cyclic voltammetry of Pt-Ru/C, Pt-Sn/C and Pt-Ru-Sn/C electrocatalysts deposited onto glassy-carbon electrode in the absence of methanol. The voltammograms of the electrocatalysts do not display a well-defined hydrogen adsorption-desorption region (0-0.4 V) as observed for Pt alloys (Spinace *et al*. 2005). The current for all the alloys in the double layer region (0.4-0.8 V vs. Ag/AgCl) is larger compared to pure Pt. The voltammograms behavior is characteristic of binary and ternary electrocatalysts containing transition metals (Ribeiro *et al*. 2008; Ribeiro *et al*. 2007). The current values were normalized per gram of platinum, considering that methanol adsorption and dehydrogenation occur only on platinum sites at room temperature (Zhou *et al*. 2003).

Fig. 6(b) shows the cyclic voltammograms of methanol oxidation under acidic conditions (1.0 M CH_3OH and 0.5 M H_2SO_4) catalyzed by Pt/C (100), Pt-Ru/C (50:50), Pt-Sn/C (50:50), Pt-Ru-Sn/C (70:10:20), Pt-Ru-Sn/C (70:15:15) and Pt-Ru-Sn/C (70:20:10) catalysts. There were three oxidation peaks when methanol CV was carried out on the Pt/C catalyst (vs. Ag/AgCl), two during the forward scan and one during the reverse scan. Table 2 summarizes the CV results of the prepared electrocatalysts including the positive peak potentials and the corresponding peak current densities of MOR. Figure 6b shows that the onset potentials of methanol electro oxidation for Pt/C (100), Pt-Ru/C (50:50), and Pt-Sn/C (50:50) are at about 0.3 V vs. Ag/AgCl. While for tri-metallic catalysts Pt-Ru-Sn/C (70:10:20), Pt-Ru-Sn/C (70:15:15) and Pt-Ru-Sn/C (70:20:10) onset potential for methanol oxidation is earlier at about 0.2 V vs. Ag/AgCl, i.e., shifted to negative potential by 0.1 V. The first electro-oxidation peak of methanol on Pt-Sn/C (50:50) is at 0.825 V (vs. Ag/AgCl), which is 0.75 V higher than that of Pt-Ru-Sn/C (70:10:20). The current density at the first peak of methanol oxidation on Pt-Ru-Sn/C (70:10:20) is 17.2 mA cm^{-2} which is higher than that on Pt-Sn/C (50:50) with a difference of 4.8 mA cm^{-2}, but less than that of Pt-Ru-Sn/C (70:15:15) and Pt-Ru-Sn/C (70:20:10). The Pt-Ru-Sn/C (70:20:10) shows highest peak current density (34.5 mA cm^{-2}) at 0.8 V peak potential, and hence possesses highest catalytic activity towards methanol oxidation among all the catalysts prepared. Pt-Ru-Sn/C (70:15:15) shows higher current density than Pt-Sn/C (50:50), Pt-Ru-Sn/C (70:10:20) and Pt-Ru/C (50:50) catalysts, indicating that Pt-Ru-Sn/C (70:15:15) is also a promising catalyst for methanol electro-oxidation.

Pure Pt/C catalyst (Fig. 6(b)) does not behave as a very good anode for methanol electro-oxidation due to its poisoning by strongly adsorbed intermediates such as CO_{ads}. However, the introduction of Ru and Sn promotes the electrocatalytic activity. On the other hand, the addition of

Table 2 CV results of Pt/C, Pt-Ru/C, Pt-Sn/C and Pt-Ru-Sn/C electrocatalysts at room temperature

Catalyst	Scan rate 0.5 Vs^{-1}	
	Positive peak potential (V vs. Ag/AgCl)	Peak current density (mA cm^{-2})
Pt/C (100)	0.795	8.5
Pt-Sn/C (50:50)	0.825	12.4
Pt-Ru/C (50:50)	0.815	13.1
Pt-Ru-Sn/C (70:10:20)	0.750	17.2
Pt-Ru-Sn/C (70:15:15)	0.760	23.6
Pt-Ru-Sn/C (70:20:10)	0.800	34.5
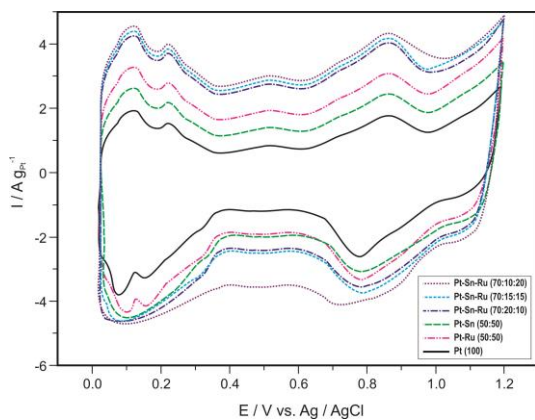
Fig. 6(a) Cyclic voltammetry of Pt/C (100), Pt-Ru/C (50:50), Pt-Sn/C (50:50), Pt-Ru-Sn/C (70:10:20), Pt-Ru-Sn/C (70:15:15) and Pt-Ru-Sn/C (70:20:10) electrocatalysts in 0.5 M H_2SO_4 at room temperature with a scan rate of 0.5 Vs^{-1}

Fig. 6(b) Cyclic voltammetry of Pt/C, Pt-Ru/C, Pt-Sn/C and Pt-Ru-Sn/C electrocatalysts in 0.5 M H_2SO_4 and 1.0 M methanol at room temperature with a scan rate of 0.5 Vs^{-1}
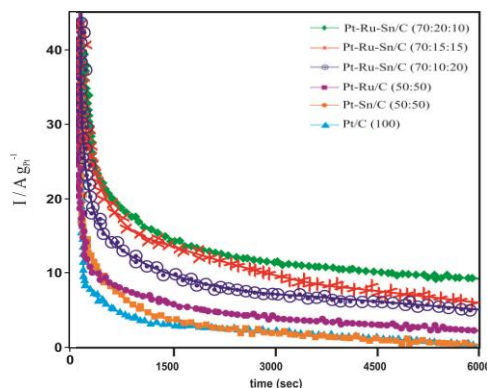
Fig. 7 Chronoamperometry of Pt/C, Pt-Ru/C, Pt-Sn/C, and Pt-Ru-Sn/C electrocatalysts at room temperature

Ru to Pt (Pt-Ru/C) had a little effect, whereas addition of Sn to Pt-Ru greatly enhanced the electrocatalytic activity. The superior activity of the ternary Pt-Ru-Sn/C electrocatalysts can be attributed to the modification of electronic properties of platinum and to the presence of stannic oxide species resulting in a combination of electronic effect and bifunctional mechanism.

3.2.2 Chronoamperometry (CA)

The Pt-Ru/C, Pt-Sn/C, and Pt-Ru-Sn/C electrocatalysts performances for methanol oxidation were studied by chronoamperometry (CA) at 0.4 V for 2 h, to evaluate both the electrocatalytic activity of the catalysts and the poisoning of the active surface under continuous operation conditions. Fig. 7 shows representative chronoamperograms obtained for the different electrocatalysts whose current densities were normalized by Pt mass. During the first five minutes, there was a sharp decrease in the current density and after some time, it becomes relatively stable. This behavior can be explained assuming that initially the active sites are free from adsorbed

methanol molecules, but a new adsorption of methanol molecules is a function of the liberation of the active sites by methanol oxidation and intermediate species formed during the first minutes, which are responsible for poisoning of the catalytic sites (Biegler *et al*. 1971).

The ternary Pt-Ru-Sn/C (70:10:20), Pt-Ru-Sn/C (70:15:15) and Pt-Ru-Sn/C (70:20:10) electrocatalysts gave higher current than the binary Pt-Ru/C (50:50) and Pt-Sn/C (50:50) electrocatalysts. Higher current obtained for the ternary electrocatalysts may be explained by the operation of a beneficial synergistic effect between Sn and Ru. This may indicate an increase in structural defects or roughness, making the ternary electrocatalysts better candidates for methanol electro-oxidation. Furthermore, the addition of Ru to the Pt-Sn alloy electrocatalysts can lead to an increase in the surface oxophilic character, thus increasing the Sn-O bond strength and the acidity of the Sn-OH sites, which can favor methanol electro oxidation at lower potentials (Chen *et al*. 2001). On the other hand, Ru atoms may disturb the Pt-Sn sites and orbital symmetries, thus affecting the orbital spatial distribution and the methanol electro-oxidation rate (Woodward *et al*. 1965). (Cunha *et al*. 2011) pointed out the presence of the oxophilic metals such as Ru and Sn in the composition of the Pt-based electrocatalysts enhances methanol oxidation. These results were similar to the obtained by (Neto *et al*. 2007) and using Pt-Ru/C, Pt-Sn/C, and Pt-Ru-Sn/C electrocatalysts prepared by a similar procedure but different from those reported by (Antolini *et al*. 2003), and (Lamy *et al*. 2004). These observations suggest that the performance of Pt-Ru-Sn/C electrocatalysts depends greatly on its atomic ratios and its preparation procedure.

3.3 Single cell test

The Pt/C (100), Pt-Ru/C (50:50), Pt-Sn/C (50:50), Pt-Ru-Sn/C (70:10:20), Pt-Ru-Sn/C (70:15:15) and Pt-Ru-Sn/C (70:20:10) catalysts were evaluated as anode catalysts for methanol electro-oxidation by single membraneless methanol fuel cell (MLMFC), and the data are presented in Fig. 8. When Pt/C (100) was used as the anode catalyst, the performance of single cell was poor. The open-circuit potential (OCP) was 0.54 V, far less than the reversible OCP (1.145 V) (Antolini *et al*. 2003), which was mainly attributed to poor catalytic activity towards methanol electro-
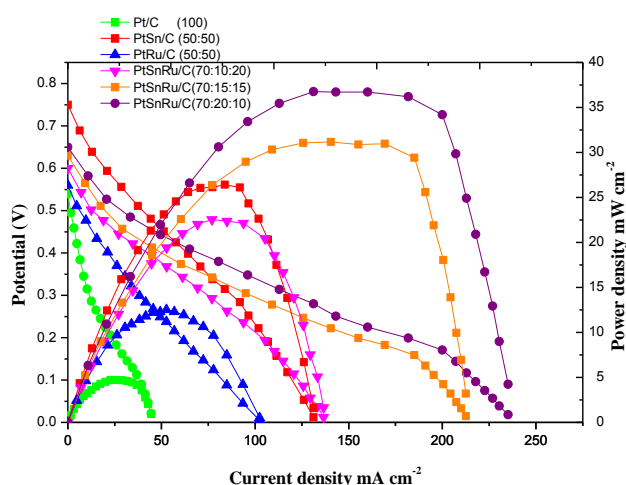
Fig. 8 Polarization and power density curves of different catalyst at 2 mg cm^{-2} catalyst loading on anode and cathode at room temperature

Table 3 Summary of performance of single fuel cell tests using (2 mg cm^{-2} catalyst loading, 40 wt% catalyst on carbon)

Anode Catalysts	Open circuit voltage (mV)	Maximum powesr density (mW cm^{-2})	Current density at maximum power density (mA cm^{-2})
Pt/C (100)	0.54	4.7	44.5
Pt-Ru/C (50:50)	0.56	12.5	102.4
Pt-Sn/C (50:50)	0.75	26.4	131.2
Pt-Ru-Sn/C (70:10:20)	0.60	22.5	136.6
Pt-Ru-Sn/C (70:15:15)	0.63	31.2	212.5
Pt-Ru-Sn/C (70:20:10)	0.65	36.5	235.1

oxidation. The maximum output power density for Pt/C (100) is 4.7 mW cm^{-2}. The results of MLMFC adopting to different catalysts are summarized in Table 3. When the current was normalized to the geometric area of single cell, it was observed that the cell performance of Pt-Ru-Sn/C (70:20:10) catalyst was better than other catalysts. In the low current discharging region, the power drawn from single cell was almost the same for all catalysts except Pt-Ru/C (50:50) and Pt/C (100). However, as the voltage reach around 0.3 V Pt-Ru-Sn/C (70:20:10) started drawing more current in comparison to others. The cell voltage of Pt-Ru-Sn/C (70:20:10) at a current density of 50 mA cm^{-2} was 0.5 V which was 0.55 V higher than the Pt-Sn/C (50:50) catalyst, although the open-circuit potential for Pt-Sn/C (50:50) catalyst was 0.75 V higher than for Pt-Ru-Sn/C (70:20:10) (0.65 V). In addition, there was a rapid initial fall in cell voltage for all catalysts, which was due to the slow initial methanol electro-oxidation reaction at the electrode surface. After an initial drop of 0.5 V the change in slope of the polarization curve for Pt-Ru-Sn/C (70:20:10) decreased, and it started drawing more current. This is attributed to the more effective catalytic ability of Pt-Ru-Sn/C (70:20:10), once the methanol electro-oxidation reaction being initiated. Based on peak power density drawn from single cell, Pt-Ru-Sn/C (70:20:10) is the best anode catalyst with peak power density value of 36.5 mW cm^{-2}.

The addition of Ru is conducive to breaking of C-C bonds in Pt-Ru-Sn/C (70:20:10), but the lesser percentage of Ru and higher percentage of Sn in Pt-Ru-Sn/C (70:15:15) and Pt-Ru-Sn/C (70:10:20) blocks the further oxidation of intermediates. This may be due to adsorption of the intermediates on the active sites of the catalysts. In the tri-metallic combinations of Pt, Sn, and Ru, the addition of Sn increases the cell performances. The addition of Sn is clearly enhancing the methanol oxidation reaction as observed from the polarization curves that the electrocatalysts containing Sn shows higher open circuit voltage. Pt-Sn/C (50:50) (Sn 50 wt.%), Pt-Ru-Sn/C (70:10:20) (Sn 20 wt.%), Pt-Ru-Sn/C (70:15:15) (Sn 15 wt.%) and Pt-Ru-Sn/C (70:20:10) (Sn 10 wt.%) showed OCV of 0.75 V, 0.60 V, 0.63 V and 0.65 V respectively in comparison to Pt-Ru/C (50:50) and Pt/C (100) which showed OCV of 0.56 V and 0.54 V, respectively. The comparison of both the bimetallic catalysts showed that peak power density of Pt-Sn/C (50:50) (26.4 mW cm^{-2}) was higher than the Pt-Ru/C (50:50) (12.5 mW cm^{-2}). It is seen that for Pt-Ru-Sn/C combination containing 10, 15, and 20 atomic ratios of Sn, the peak power densities are 22.5, 31.2 and 36.5 mW cm^{-2}, respectively. This indicates that only a small amount of Sn in Pt-Sn-Ru/C catalyst helps in electro-oxidation of methanol. Even under fuel cell working conditions, the best performance is achieved with lower Sn atomic ratios. Similar results were observed by (Ribeiro *et al*. 2008) for alcohol oxidation using catalysts prepared by the Pechini-Adams modified method.

4. Conclusions

A microscale membraneless methanol fuel cell (MLMFC) was fabricated with Pt-Ru-Sn/C eletrocatalysts and its performance was evaluated under different operating conditions. Standard microfabrication techniques were used to develop this device. In this work, we observed that the alcohol-reduction process could be effectively used for the preparation of Pt-Ru/C, Pt-Sn/C and Pt-Ru-Sn/C eletrocatalysts for methanol oxidation. The *X*-ray diffractograms of the Pt-Ru/C electrocatalyst showed a typical fcc structure of the Pt alloys. The Pt-Sn/C and Pt-Ru-Sn/C electrocatalysts showed a typical fcc structure of platinum alloys in the presence of a separated SnO_2 phase. The Pt metal was the predominant material in all the samples, with peaks attributed to the face-centered cubic (fcc) crystalline structure. EDX analysis indicated that the experimental composition is in agreement with the nominal composition of the catalyst, which confirm the formation Pt-Ru-Sn/C, Pt-Ru/C and Pt-Sn/C metal catalysts having typical Pt crystalline structure and the formation of Pt-Sn alloy. Cyclic voltammetry results showed that Pt-Ru-Sn/C (70:20:10) is more active in methanol electro-oxidation than other catalysts. The onset potential for this reaction was found to be 0.2 V vs. Ag/AgCl, which suggests that activation, takes place at the electrode surface by a ligand effect. Chronoamperometry results showed that the ternary electrocatalysts gave higher current than the binary catalysts at steady condition. The enhanced methanol oxidation activity by the ternary Pt-Ru-Sn/C catalyst was mainly ascribed to the synergistic effect between Ru and Sn, and to the smaller particle size. In this work, for the first-time carbon-supported binary Pt-Ru/C, Pt-Sn/C and ternary Pt-Ru-Sn/C anode catalysts were successfully tested in a single membraneless methanol fuel cell using 1.0 M methanol as the fuel and 0.1 M sodium percarbonate as the oxidant in the presence of 0.5 M H_2SO_4 as the electrolyte. Based on peak power density drawn from a single cell, Pt-Ru-Sn/C (70:20:10) is the best anode catalyst with peak power density value of 36.5 mW cm^{-2} among the catalysts tested.

References

Antolini, E. (2003), "Formation of carbon-supported PtM alloys for low temperature fuel cells: a review", *Mater. Chem. and Phy.*, **78**(3), 563-573.

Arun, A., Gowdhamamoorthi, M., Kiruthika, S. and Muthukumaran, B. (2014), "Analysis of membraneless methanol fuel cell using percarbonate as an oxidant", *J. Electrochem. Soc.*, **161**(3), F311- F317.

Beyhan, S., Leger, J.M. and Kadırgan, F. (2013), "Pronounced synergetic effect of the nano-sized PtSnNi/C catalyst for ethanol oxidation in direct ethanol fuel cell", *Appl. Catal. B.*, **130**(131), 305-313.

Biegler, T., Rand, D.A.J. and Woods, R. (1971), "Limiting oxygen coverage on platinized platinum; Relevance to determination of real platinum area by hydrogen adsorption", *J. Electroanalyt. Chem.*, **29**(2), 269-277.

Carrette, L., Friedrich, K.A. and Stimming, U. (2000), "Fuel cells: principles, types, fuels, and applications", *Chem. Phys. Chem.*, **1**(4), 162-193.

Casado Rivera, E., Volpe, D.J., Alden, L., Lind, C., Downie, C., Vazquez Alvarez, T., Angelo, A.C.D., DiSalvo, F.J. and Abruna, H.D. (2004), "Electrocatalytic activity of ordered intermetallic phases for fuel cell applications", *J. Amer. Chem. Soc.*, **126**(12), 4043-4049.

Chan, K.Y., Ding, J., Ren, J., Cheng, S. and Tsang, K.Y. (2004), "Supported mixed metal nanoparticles as in low temperature fuel cells", *J. Mater. Chem.*, **14**(4), 505-516.

Chen, G., Delafuente, D.A., Sarangapani, S. and Mallouk, T.E. (2001), "Combinatorial discovery of bifunctional oxygen reduction-water oxidation electrocatalysts for regenerative fuel cells", *Catal. Today*, **67**(4), 341-55.

Choban, E.R., Markoski, L.J., Wieckowski, A. and Kenis, P.J.A. (2004), "Microfluidic fuel cell based on laminar flow", *J. Power Sour.*, **128**(1), 54-60.

Choban, E.R., Waszczuk, P. and Kenis, P.J.A. (2005), "Characterization of Limiting Factors in Laminar Flow-Based Microfuel Cells", *Electrochem. Solid-State Lett.*, **8**(7), A348-A352.

Cotton, F.A. and Wilkinson, G. (1988), *Advanced inorganic chemistry*, Wiley Interscience, New York.

Colmati, F., Antolini, E. and Gonzalez, E.R. (2007), "Ethanol oxidation on a carbon-supported $Pt_{75}Sn_{25}$ electrocatalyst prepared by reduction with formic acid: effect of thermal treatment", *Appl. Catal. B: Environ.*, **73**(1-2), 106-115.

Cunha, E.M., Ribeiro, J., Kokoh, K.B. and de Andrade, A.R. (2011), "Preparation, characterization and application of Pt-Ru-Sn/C trimetallic electrocatalysts for ethanol oxidation in direct fuel cell", *Int. J. Hydrogen Energy.*, **36**(17), 11034-11042.

Ferrigno, R., Stroock, A.D., Clark, T.D., Mayer, M. and Whitesides, G.M. (2002), "Membraneless vanadium redox fuel cell using laminar flow", *J. Amer. Chem. Soc.*, **124**(44), 12930-12931.

Gasteiger, H.A., Markovic, N., Ross, P.N. and Cairns, E.J. (1993), "Methanol electrooxidation on well-characterized platinum-rutheniumbulk alloys", *J. Phys. Chem.*, **97**(46), 12020-12029.

Gowdhamamoorthi, M., Arun, A., Kiruthika, S. and Muthukumaran, B. (2014), "Perborate as novel fuel for enhanced performance of membraneless fuel cells", *Ionics.*, **20**(12), 1723-1728.

Jayashree, R.S., Yoon, S.K., Brushett, F.R., Lopez-Montesinos, P.O., Natarajan, D., Markoski, L.J. and Kenis, P.J.A. (2010), "On the performance of membraneless laminar flow-based fuel cells", *J. Power Sour.*, **195**(11), 3569-3578.

Jiang, L., Sun, G., Sun, S., Liu, J., Tang, S., Li, H., Zhou, B. and Xin, Q. (2005), "Structure and chemical composition of supported Pt-Sn electrocatalysts for ethanol oxidation", *Electrochimica Acta*, **50**(27), 5384-5389.

Karunakaran, C. and Kamalam, R. (2002), "Structure-reactivity correlation of anilines in acetic acid", *J. Organic Chem.*, **67**(4), 1118-1124.

Lamy, C., Rousseau, S., Belgsir, E., Coutanceau, C. and Léger, J.M. (2004), "Recent progress in the direct ethanol fuel cell: development of new platinum-tin electrocatalysts", *Electrochimica Acta*, **49**(22-23), 3901-3908.

Amani, M., Kazemeini, M., Hamedanian, M., Pahlavanzadeh, H. and Gharibi, H. (2015), "Investigation of methanol oxidation on a highly active and stable Pt-Sn electrocatalyst supported on carbon-polyaniline composite for application in a passive direct methanol fuel cell", *Mater. Res. Bul.*, **68**, 166-178.

Neto, A.O., Dias, R.R., Tusi, M.M., Linardi, M. and Spinace, E.V. (2007), "Electro-oxidation of methanol and ethanol using PtRu/C, PtSn/C and PtSnRu/C electrocatalysts prepared by an alcohol-reduction process", *J. Power Sour.,* **166**(1), 87-91.

Radmilovic, V., Gasteiger, H.A. and Ross, P.N. (1995), "Structure and chemical composition of a supported Pt-Ru electrocatalyst for methanol oxidation", *J. Catal.*, **154**(1), 98-106.

Ribeiro, J., dos Anjos, D.M., Kokoh, K.B., Coutanceau, C., Leger, J.M., Olivi, P., de Andrade, A.R. and Tremiliosi-Filho, G. (2007), "Carbon-supported ternary PtSnIr catalysts for direct ethanol fuel cell", *Electrochimica Acta*, **52**(24), 6997-7006.

Ribeiro, J., dos Anjos, D.M., Leger, J.M., Hahn, F., Olivi, P., de Andrade, A.R., Tremiliso-Filho, G. and Kokoh, K.B. (2008), "Effect on W on PtSn/C catalysts for ethanol electrooxidation", *J. Appl. Electrochem.*, **38**(5), 653-62.

Song, S.Q., Zhou, W.J., Zhou, Z.H., Jiang, L.H., Sun, G.Q., Zin, Q., Leontidis, V., Kontou, S. and Tsiakaras, P. (2005), "Direct ethanol PEM fuel cells: The case of platinum based anodes", *Int. J. Hydrogen Energy*, **30**(9), 995-1001.

Spinace, E.V., Neto, A.O., Vasconcelos, T.R.R. and Linardi, M. (2004), "Electro-oxidation of ethanol using PtRu/C electrocatalysts prepared by alcohol-reduction process", *J. Power Sour.*, **137**(1), 17-23.

Spinace, E.V., Linardi, M. and Neto, A.O. (2005), "Co-catalytic effect of nickel in the electro-oxidation of ethanol on binary Pt-Sn electrocatalysts", *Electrochem. Commun.*, **7**(4), 365-369.

Woodward, R.B. and Hoffman, R. (1965), "Selection rules for concerted cycloaddition reactions", *J. Amer. Chem. Soc.*, **87**(9), 2046-2048.

Xiong, L., Kannan, A.M. and Manthiram, A. (2002), "Pt-M (M=Fe, Co, Ni and Cu) electrocatalysts synthesized by an aqueous route for proton exchange membrane fuel cells", *Electrochem. Commun.*, **4**(11), 898-903.

Yajima, T., Uchida, H. and Watanabe, M. (2004), "In-situ ATR-FTIR spectroscopic study of electro-oxidation of methanol and adsorbed CO at Pt-Ru alloy", *J. Phys. Chem. B.*, **108**(8), 2654-2659.

Zhou, Z., Wang, S., Zhou, W., Wang, G., Jiang, L., Li, W., Shuquin, S., Liu, J., Sun, G. and Xin, Q. (2003), "Novel synthesis of highly active Pt/C cathode electrocatalyst for direct methanol fuel cell", *Chem. Commun.*, (3), 394-395.

Zhou, W.J., Song, S.Q., Li ,W.Z., Zhou, Z.H., Sun, G.Q. and Zin, Q. *et al.* (2005), "Direct ethanol fuel cells based on PtSn anodes: the effect of Sn content on the fuel cell Performance", *J. Power Sour.*, **140**(1), 50-58.

CC